

Corrosion inhibition effect of Cannabis sativa leaves extracts on N80 steel in 15% HCl solution: Experimental, Surface and Computational studies

Dengdeng Zheng*, Guojie Wang

School of Engineering, Fujian Jiangxia University, Fuzhou, Fujian 350108, China

*E-mail: kittynew1@163.com

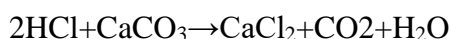
Received: 15 January 2021 / Accepted: 6 March 2021 / Published: 31 March 2021

The present paper reveals the corrosion inhibition estimation of Cannabis sativa (CS) extract on N80 steel in 15% HCl. EIS results suggests that charge transfer resistance (R_{ct}) increases as the CS extract increases concentration. PDP result suggests that CS extract acts as mixed type inhibitor. The result of weight loss reveals the maximum inhibition efficiency value of 97.53% at g/L. The adsorption of CS extract obeys Langmuir isotherm model. Scanning electron microscope (SEM) suggests smooth surface of N80 steel with the addition of CS extract. Density functional theory (DFT) suggests that protonated form of CS has more adsorption ability than neutral form. The Molecular dynamic simulation (MD) results suggest the higher value of adsorption energy for protonated form as compared to neutral form.

Keywords: N80 steel; HCl; Electrochemical study; DFT; MD

1. INTRODUCTION

The production of the crude oil from the reservoir is not a continuous process due to the depletion of the oil well. Thus, suitable techniques are used which can enhance the oil recovery from the depleted well. The most commonly used technique in this regard is the oil well stimulation or acidization. The purpose of the acidization technique is to improve the oil flow from the depleted well by opening the new channels or making more porous the already existing channels presenting in the rock formation [1]. The acidizing process required commonly hydrochloric acid (HCl) in the range of 5-28% concentration for the carbonate reservoir [2]. The commonly occurring reaction of HCl with the carbonate rock is as follows:



In petroleum industry, commonly used carbon alloy is N80 steel because of the economic value and easy availability [3, 4]. During the acidizing process commonly a solution of 15% HCl has been inserted via N80 tubular steel. However, this leads to encounter in the deterioration of N80 steel that leads to enormous financial loss [5-7].

The most practical way to overcome from the corrosion during acidizing process is the application of corrosion inhibitors [8-14]. The most commonly used corrosion inhibitors are the organic compounds. The efficient organic compounds contains certain nucleophilic regions like conjugated double, triple bond and electronegative groups. These regions helps the inhibitor to bind strongly onto the metal surface through π -interactions [15]. In addition, the further enhancement of adsorption of inhibitor molecules takes place by the presence of aromatic rings along with nitrogen, sulfur, phosphorus, and oxygen [16-20]. The surface area covered by the inhibitor molecules and planarity also contribute a major part during the adsorption process, and enhancing the effectiveness of the inhibitor molecules [21].

It is important to note that application of some chemicals as corrosion inhibitors causes harmful impacts over the environment due to their toxicity, unable to biologically degrade. However, addition of plant extracts that contains electron rich phytochemicals as corrosion inhibitors can overcome these issues [22, 23, 24]. Literature analysis suggests numerous natural based corrosion inhibitors has been developed [25, 22, 23, 26, 27].

The theme of this research is to explore the corrosion inhibition properties of *C. sativa* (CS) leave extract for N80 steel in 15% HCl. The methodology of investigation applied is weight loss, electrochemical impedance spectroscopy (EIS) and potentiodynamic polarization (PDP). The morphological inspection of metal was done using Scanning electron microscope (SEM). The computational study of major constituent was done using density functional theory (DFT) and molecular dynamic simulation (MD).

2. EXPERIMENTAL DETAILS

2.1. Preparation of leaves extracts

The leaves of *Cannabis sativa* (CS) were dried in oven at 45 °C, and grinded to powder. Ten gram of the powder was added to 2.5 L of 15% HCl solution, and refluxed for 1 h. Thereafter, the mixture was cooled and filtered. The precipitate was dried and weighed. The extract was concentrated by evaporating the solvent and maintained its concentration to 10000 g/L. Leaves extract test solutions were prepared at concentrations of 0.1, 0.2, 0.3 and 0.5 g L. The leaves of *C. sativa* (CS) contain various water soluble chemical constituents tetrahydrocannabinol, cannabidiol, cannabinol, tetrahydrocannabivarin and cannabigerol but tetrahydrocannabinol (Fig. 1) is most abundant biologically active constituents [28, 29].

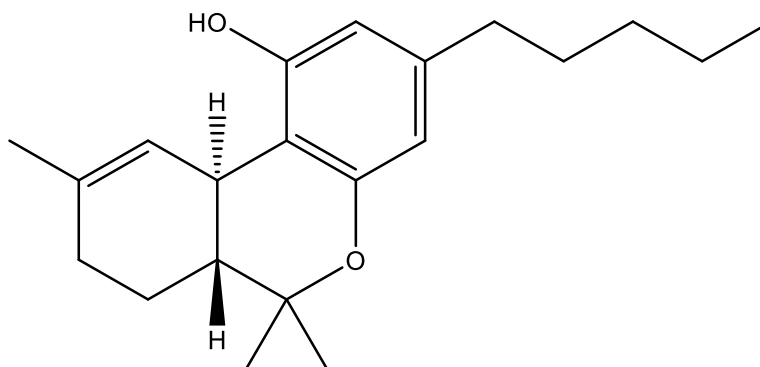


Figure 1. Structure of tetrahydrocannabinol

2.2. Metal sample and corrosive solution preparation

The N80 steel has composition of (wt.%) that includes C= 0.31%, Si= 0.19% Mn= 0.92%, P= 0.01%, S= 0.008%, Cr= 0.2% and remaining Fe. The metal samples have a dimension of 2.5 cm × 2.0 cm × 0.5 cm for weight loss experiments. The metal sample was abraded using emery papers of different grades from 120-2000. For electrochemical experiments samples of an area of 1 cm² were used. All the samples were washed using distilled water and acetone, and dried before the experiments. The aggressive medium of 15% HCl was made using analytical grade HCl (37%).

2.3. Inhibition evaluation methods

2.3.1. Weight loss method

The weight loss experiments were carried out at 308 K temperature without and with different concentrations of CS using ASTM standard [30] for 6h immersion time. The equations (1 and 2) were used for the calculation of corrosion rate (C_R) and inhibition efficiency ($\eta\%$):

$$C_R = \frac{8.76 \times 10^4 \times \Delta m}{s \times t \times \rho} \quad (1)$$

$$\eta\% = \frac{C_R - C_{R(i)}}{C_R} \times 100 \quad (2)$$

where $C_R, C_{R(i)}, \Delta m, \rho, s$ and t corresponds to corrosion rate (mm/y) without CS and with CS, metal loss, density, exposed area and immersion time in g, g cm⁻³, cm² and respectively.

2.3.2. Electrochemical methods

The tested methods used in electrochemical study include electrochemical impedance spectroscopy (EIS) and potentiodynamic polarization (PDP) using Gamry Potentiostat (reference 300) at 308 K temperature. The data fitting was done using Echem Analyst 6.0 software. The cell assembly used for the experiments includes N80 steel as working electrode, saturated calomel electrode (SCE) as reference and graphite rod as counter electrode.

The experiments of EIS were carried at OCP by applying the frequency range of 100 kHz to 0.1 Hz at amplitude of 10 mV. In PDP experiments a potential range of ± 250 mV with respect to the OCP at the scan rate of 1 mV/s was used. The calculation of inhibition efficiency (% IE) results of EIS and PDP were achieved using below equations (3,4):

$$\eta_{EIS\%} = \frac{R_{ct}^p - R_{ct}^a}{R_{ct}^p} \times 100 \quad (3)$$

$$\eta_{PDP\%} = \frac{i_{corr}^a - i_{corr}^p}{i_{corr}^a} \times 100 \quad (4)$$

where R_{ct}^p , R_{ct}^a , i_{corr}^p and i_{corr}^a are the charge transfer resistance and corrosion current density with inhibitor and devoid of inhibitor respectively.

2.3.3. Scanning electron microscope (SEM)

The surface morphological investigation using SEM was done by immersing the N80 steel samples (without and with optimum concentration CS) in 15% HCl at 308 K for 6. The operating condition for SEM was at accelerating voltage of 5 kV and 5KX magnification.

2.4. Computational analysis

The molecular structure of active constituent (tetrahydrocannabinol) in the CS extract was analyzed at 6-31 G (d, p) basis set and B3LYP correlation functions using Density Functional Theory (DFT). The Gaussian 09W software program was used to perform the calculation [31]. Some important atomic-level parameters that consist of highest occupied molecular orbital energy (E_{HOMO}), lowest unoccupied molecular orbital energy (E_{LUMO}), and energy gap (ΔE) was explored. To make the computational calculation more closely to experimental conditions, we performed the calculation in aqueous state using the help of Polarized continuum model (PCM).

2.5. Molecular Dynamics Simulation

The stimulation of neutral and protonated forms of CS active constituent (tetrahydrocannabinol) interaction with iron surface was achieved using Materials Studio software (Accelrys, Inc.). The inhibitor optimization was done by Forcite module [32]. The iron unit cell used was imported from Materials Studio. The iron cell was cleaved in hkl (110) fashion and enlarged into 10×10 supercell. Over the Fe (110) plane 30 \AA thicknesses vacuum slab was built. The corrosive solution was simulated using 491 water, 9 HCl, and 1 inhibitor molecules respectively. The metal and inhibitor interaction was simulated in the box $25 \times 25 \times 79.91 \text{ \AA}$. The adsorption energy (E_{ads}) was estimated using below equation:

$$E_{ads} = E_{Total} - (E_{surf} + E_{inh}) \quad (5)$$

Where E_{Total} is energy of metal surface and adsorbed CS molecule, E_{surf} is energy of metal surface without CS, and E_{inh} is energy of CS molecule.

3. RESULTS AND DISCUSSION

3.1. Weight loss study

The inhibition efficiency (η %) and corrosion rate (C_R) variation with the addition of different concentration of CS extract over N80 steel corrosion inhibition at 308 K are depicted in Fig. 2.

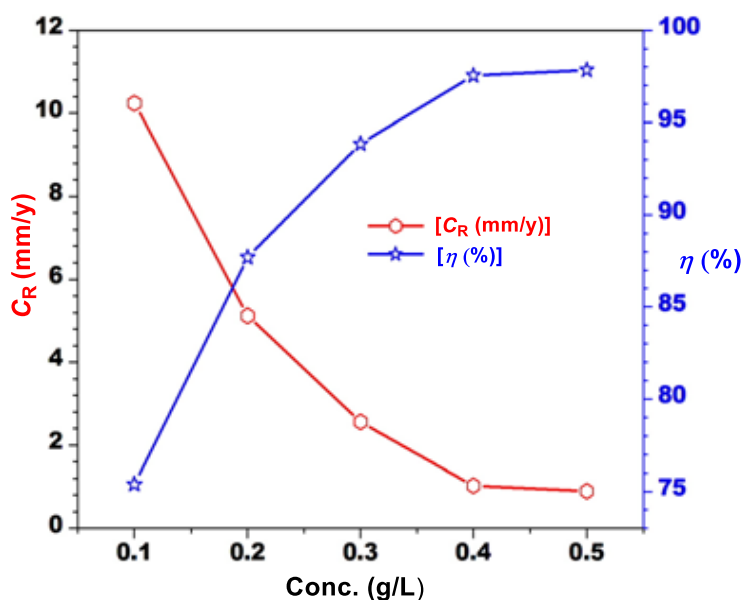


Figure 2. Variation of inhibition efficiency (η %) and Corrosion rate (C_R) of CS extract on corrosion inhibition of N80 steel in 15% HCl at 308 K temperature

The investigation of figure reveals that the values of η % and C_R increase and decreases with increasing CS extract concentration. This suggests that as CS concentration increase more number of CS extracts constituents molecules adsorbed over the metal surface and that provides more surface coverage of metals surface. The values of η % and C_R at optimum concentration (0.4 g/L) are 97.53% and 1.024 mm/y respectively. It is noteworthy that an increase in further CS concentration gives no significant impact over the values of η % and C_R . Therefore we have selected 0.4 g/L as the optimum concentration. The interaction of mains constituents can be explained on the fact that all of them consists of phenyl ring and $-\text{OH}$ as the functional groups. The π -electrons and lone pair of electrons residing over the phenyl rings and oxygen atoms can donate electrons to the empty iron orbitals and thus creates an inhibitor film barrier that prevents the insertion of acidic solution and finally protect the N80 steel from corrosion [33-35].

3.2. Adsorption isotherm

The adsorptive nature of CS molecules adsorption over the metal surface was investigated with the surface coverage (θ) values using suitable adsorption isotherm models like Langmuir, Temkin, Flory-Huggins and Frumkin at 308 K temperature. Although, out of these isotherm model only Langmuir showed the best fitting values of R^2 and slope close to 1. Langmuir adsorption isotherm model can be represented using below mathematical equation [36]:

$$\frac{C_{inh}}{\theta} = \frac{1}{K_{ads}} + C_{inh} \quad (6)$$

Where C_{inh} represents CS concentration (g/L) and K_{ads} represents equilibrium adsorption constant. The display of Langmuir, Temkin, Flory-Huggins and Frumkin isotherm models are pictorially shown in Fig. 3.

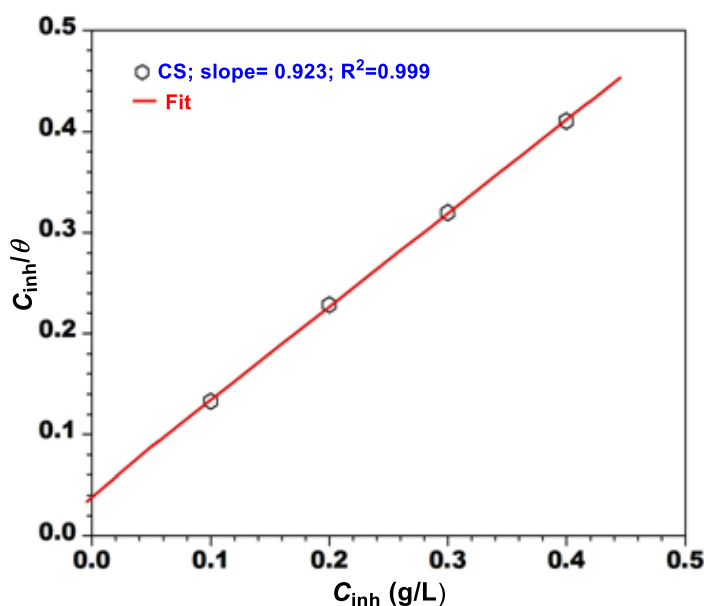


Figure 3. Langmuir isotherm for the adsorption of CS extract over N80 steel surface in 15% HCl

The value of K_{ads} was calculated using the intercept of C_{inh} and (C_{inh}/θ) plot. The value of free energy change of adsorption ΔG_{ads} was estimated using the values of K_{ads} with the application of below equation:

$$\Delta G_{ads} = -2.303RT \log(1000K_{ads}) \quad (7)$$

Where R, T and 1000 shows the values of universal gas constant, absolute temperature and concentration of water molecules. The K_{ads} and ΔG_{ads} values are 24.3 L/g and -25.87 kJ/mol respectively. The calculated value of K_{ads} is high that suggest the strong interaction among the CS extract molecules and N80 steel surface. The spontaneous adsorption nature of CS extract is due to the obtained negative value of ΔG_{ads} [37]. Additionally, the calculated values of ΔG_{ads} are coming in the

range of physical and chemical adsorption that reveals towards the mixed mode of inhibition adsorption action [38].

3.3. Electrochemical studies

3.3.1. Electrochemical Impedance (EIS)

Fig. 4a corresponds to the fitted Nyquist plots in 15% HCl solution at 308 K temperature without and with different concentrations of CS extract. The examination of figure suggests the presence of depressed semi-circle that is because of surface inhomogeneity.

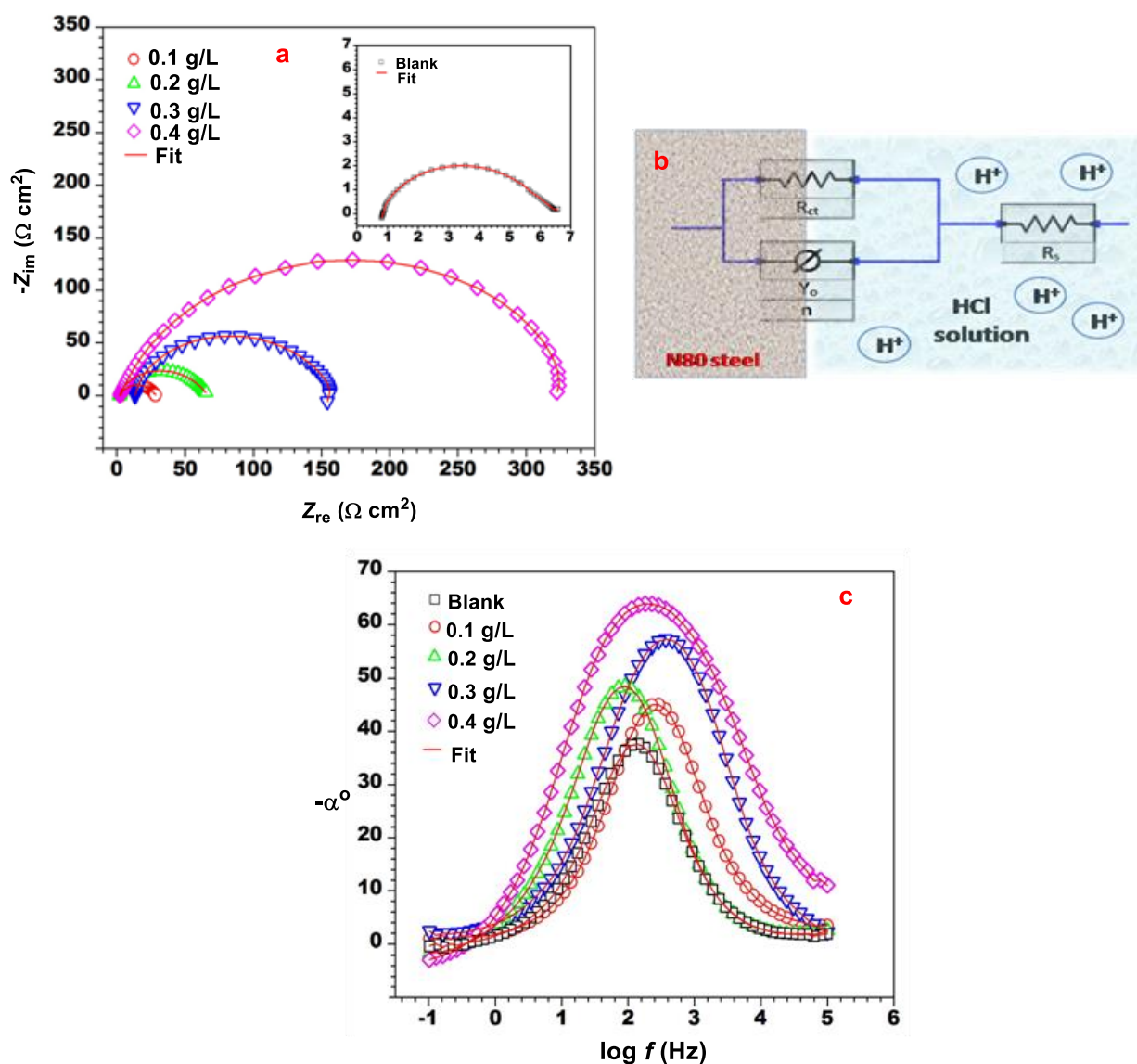


Figure 4. (a) Nyquist plots (b) Equivalent circuit used (c) Phase angle plots of N80 steel in 15% HCl without and with different concentrations of CS extract at 308 K.

The semi-circle appearance further corresponds towards the capacitive behavior of N80 steel. Additionally, with increasing CS extract concentration the diameter of semi-circle increased that suggests the increase in the charge transfer resistance (R_{ct}) of N80 steel. The exporting of data from the Nyquist was achieved using the equivalent circuit (Fig. 4b). The constricting elements of this circuit are constant phase element (CPE), charge transfer resistance (R_{ct}), and solution resistance (R_s). The calculation of double-layer capacitance (C_{dl}) was done using the equation (7):

$$C_{dl} = (Y_o R_{ct}^{1-n})^{1/n} \quad (8)$$

The data of some important impedance parameters are tabulated in Table 1.

Table 1. Electrochemical impedance parameters of N80 steel corrosion in 15% HCl at 308 K

C_{inh} (g/L)	R_s (Ωcm^2)	R_{ct} (Ωcm^2)	Y_0 ($\Omega^{-1}\text{s}^n/\text{cm}^2$)	n	C_{dl} $\mu\text{F}/\text{cm}^2$	η (%)
Blank	0.79	5.694	332.2	0.761	3553.0	--
0.1	1.16	27.71	217.4	0.794	2080.2	79.4
0.2	1.05	63.04	173.4	0.825	1246.6	90.9
0.3	12.9	141.73	112.4	0.867	495.9	95.9
0.4	1.23	319.71	82.5	0.887	301.7	98.2

As per table, the increasing concentration of CS extract the values of R_{ct} and C_{dl} were increased and decreased respectively. The obtained value of R_{ct} at optimum concentration (0.4 g/L) is 319.71 Ωcm^2 . The increasing values of R_{ct} with increasing CS extract concentration reveals the adsorption of CS extract molecules over the N80 steel surface [39]. Additionally, with the increasing concentration of CS extract the values of inhibition efficiency also increased and achieved the value of 98.2% at 0.4 g/L. In the plots of Phase angle (Fig. 4c) the values of phase angles increased with the increasing CS extracts concentration with respect to the blank (-37.39). This increase is due to the adsorption CS extract molecules onto the N80 steel surface that reduces the metal dissolution. The maximum value of phase angle at an intermediate frequency is -63.86 at 0.4 g/L CS extract.

3.3.2. Potentiodynamic polarization (PDP) analysis

The curve of PDP without and with different concentration of CS extract is represented in Fig. 5.

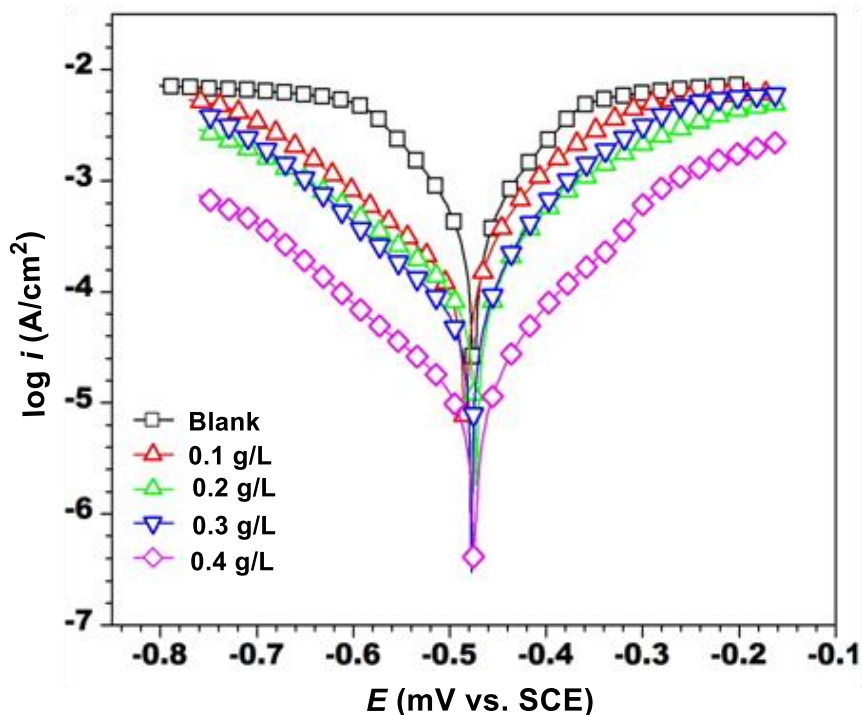


Figure 5. PDP curves of N80 steel in 15% HCl without and with different concentrations of CS extract at 308 K.

The electrochemical reactions parameters are obtained by the extrapolation of Tafel curves and are given in Table 2.

Table 2. Potentiodynamic polarization parameters of N80 steel in 15% HCl at different concentration of extracts at 308 K

C_{inh} (g/L)	E_{corr} (mV/SCE)	i_{corr} ($\mu\text{A}/\text{cm}^2$)	η (%)
Blank	-0.473	247.8	--
0.1	-0.481	59.4	76.0
0.2	-0.470	32.5	86.8
0.3	-0.476	22.8	90.7
0.4	-0.472	5.0	97.9

The results of Table suggests the as the CS extract concentration increases the corrosion current density values decreased that eventually increased the inhibition efficiency. The maximum increase in inhibition efficiency and corrosion current density values is 97.9% and $5.0\mu\text{A}/\text{cm}^2$ respectively. The shifts in the E_{corr} values with addition of CS extract are in both negative and positive direction with respect to blank. Therefore, in the present investigation the CS extract is classified as mixed type inhibitor. The increasing concentration of CS extract affects both anodic and cathodic Tafel slopes values that suggest the modification in the corrosion reaction kinetics. The changes in the values of β_c

as compared to blank (without CS extract) causes change the reaction kinetics of hydrogen evolution and this is because of the diffusion or barrier effect [40]. In the same way, β_a values change is due to the initial adsorption of CS extract molecules over the N80 steel surface that blocks the anodic reactions without changing the mechanism of anodic reactions [41].

3.4. Scanning Electron microscopy (SEM)

The surface modifications of metal surfaces without and with addition of CS extracts are shown in Fig. 6a, b.

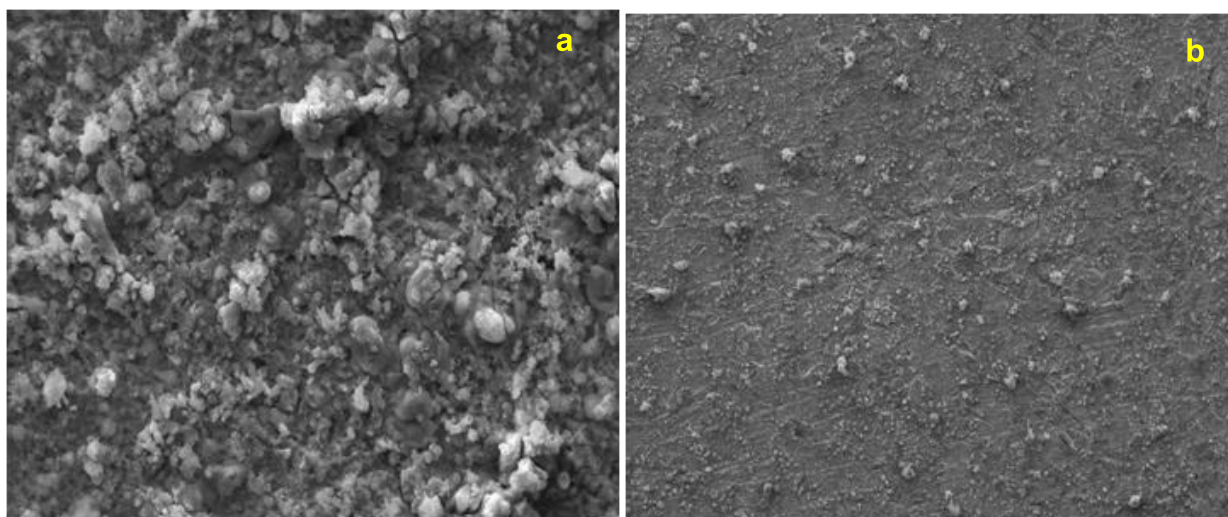


Figure 6. SEM images of N80 steel in 15% HCl at 308 K (a) without CS extracts (b) with optimum concentration (0.4 g/L) of CS extract without and with different concentrations of CS

The image of metal without the CS extract addition represents the severely damaged surface due to the corrosive attack of 15% HCl (Fig. 6a). However, addition of CS extract into the corrosive medium (15% HCl) causes to decrease the destructive attack of corrosive medium over the N80 steel surface that results in the smoother N80 steel surface (Fig. 6b).

3.5. Quantum chemical calculation

The reactivity of inhibitor molecules can be defined on the basis of frontier molecular orbital energies (FMOs) that consists of highest occupied molecular orbital (E_{HOMO}), lowest unoccupied molecular orbital (E_{LUMO}) and energy gap (ΔE). HOMO and LUMO energies correspond to the donation and acceptance of electrons respectively. The orbital distributions of FMOs for both neutral and protonated forms of active constituents of CS like tetrahydrocannabinol are shown in Fig. 7.

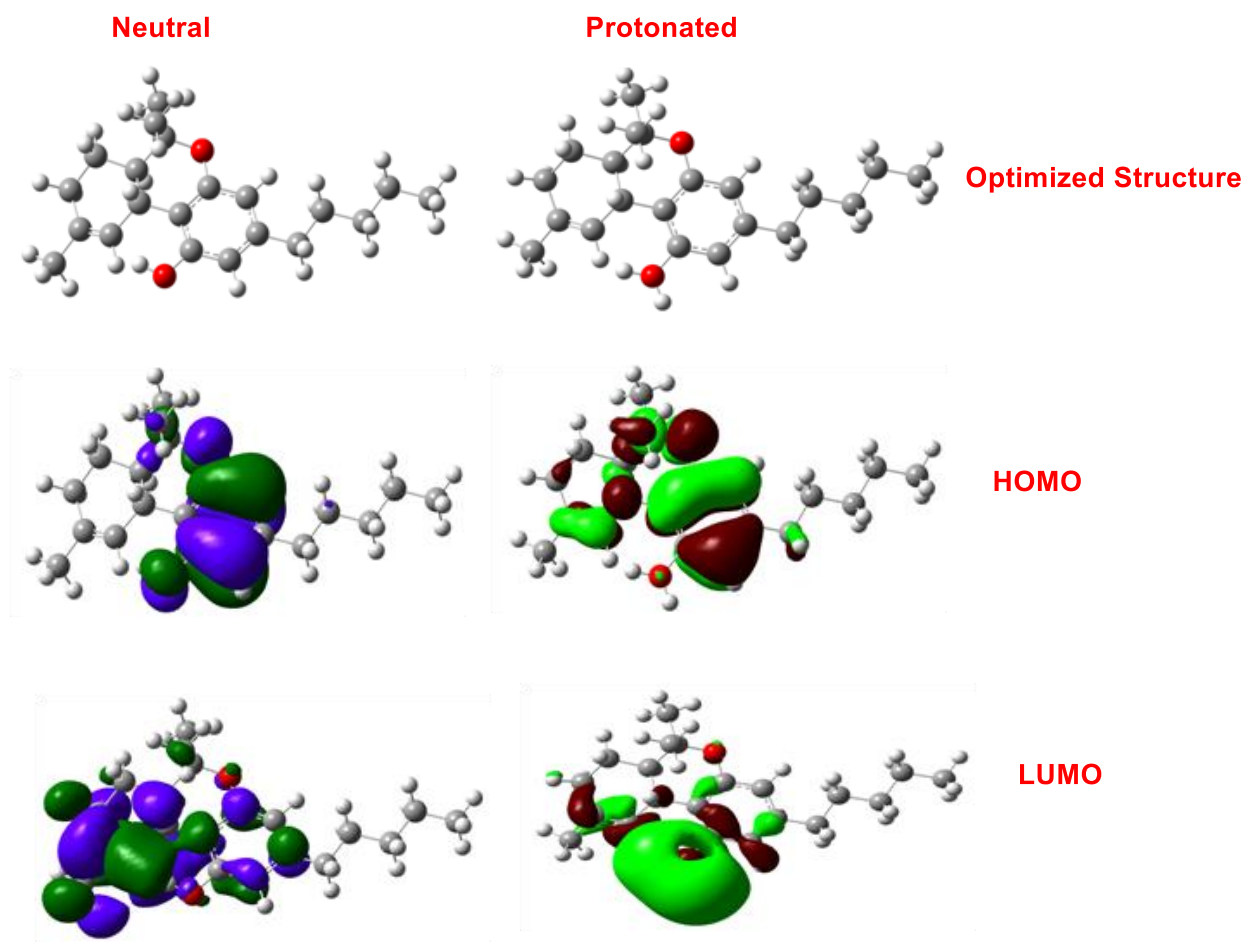


Figure 7. Optimized, HOMO and LUMO images of active constituent of CS (tetrahydrocannabinol) using DFT

In both neutral and protonated forms HOMO and LUMO are distributed over the pyran, phenyl rings and OH groups. The energy comparison of HOMO and LUMO orbitals suggests that neutral form of E_{HOMO} has higher energy as compared to protonated form. However, E_{LUMO} of protonated form is lower than neutral form (Table 3).

Table 3. Quantum chemical calculation using DFT methods

Inhibitor	E_{HOMO}	E_{LUMO}	ΔE
CS neutral	-5.310	0.106	5.416
CS protonated	-9.297	-4.482	4.815

This reveals that neutral form has more electron donation than protonated form [42]. However, the values of energy gap (ΔE) of protonated form are lower as compared to neutral form. This observation suggests that protonated form has more adsorption ability than neutral form [43].

3.6. Molecular dynamic simulation (MD)

The equilibrium adsorption configurations of both neutral and protonated forms of active constituents of CS including tetrahydrocannabinol over Fe (110) surface are shown in Fig. 8.

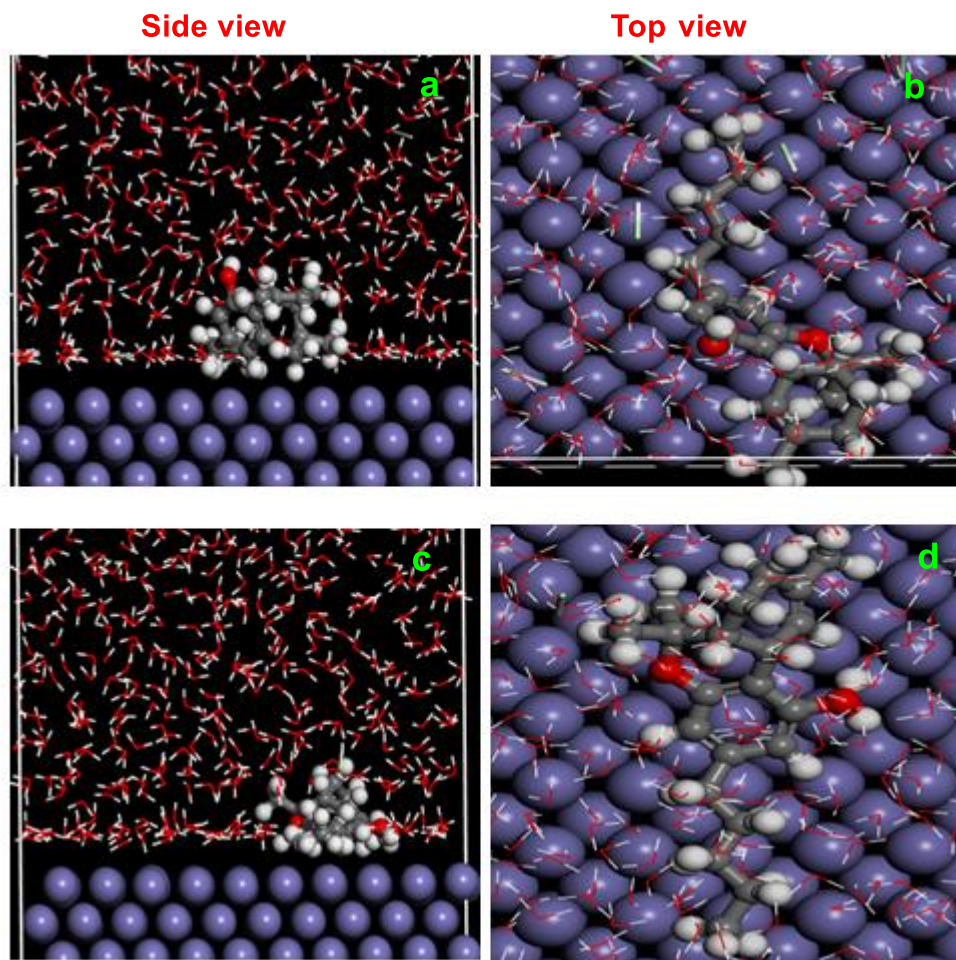


Figure 8. Side and top views of the final adsorption of neutral and protonated forms of active constituents of CS (tetrahydrocannabinol) on Fe(110) surface in solution

In protonated form the inhibitor molecules adsorbed in parallel manner over the iron surface. However, in neutral form inhibitor adsorption is not in parallel as compared to protonated form. These molecular adsorption configuration of inhibitor molecule provide the higher value of adsorption energy (E_{ads}) (-7554.5 kcal/mol) for protonated form as compared to the neutral form (-7435.5 kcal/mol). Although, the values of adsorption energy (E_{ads}) in both neutral and protonated forms are very high that results in stronger of CS extract over the iron surface [44-46]. Thus, the MD result supports both the results of experimental and quantum chemical calculations.

4. CONCLUSIONS

Following conclusion has been drawn on the basis of experimental and computational investigation:

1. The leaves extract of CS is efficient environmentally friendly corrosion inhibitor for N80 steel in 15% HCl.
2. The value of inhibition efficiency increases as the CS concentration increases and maximum efficiency is 97.53% at optimum concentration (0.4 g/ L).
3. The CS adsorption takes place through the Langmuir adsorption isotherm model.
4. The result of EIS suggests the increase in the charge transfer resistance.
5. The result of PDP reveals mixed-type of CS extract adsorption over the N80 steel surface.
6. The DFT results suggest that protonated form of CS has more adsorption ability than neutral form.
7. The MD results suggest the higher value of adsorption energy for protonated form as compared to neutral form.

ACKNOWLEDGEMENTS

Authors are thankful to the Fujian Provincial Department of Education Project JAT190460, Fujian Natural Science Foundation University Joint Fund Project-2020J01939 and Fujian Science and Technology Planning Project-2019H6025. The author also thankful Dr. K.R .Ansari for performing DFT and MD study.

References

1. Devold, H., Oil and Gas Production Handbook: an Introduction to Oil and Gas Production. Lulu. Com, 2013
2. Finšgar, M., Jackson, J. Application of corrosion inhibitors for steels in acidic media for the oil and gas industry: a review. *Corros. Sci.* 86 (2014) 17
3. A. Singh, Y. Lin, W. Liu, D. Kuanhai, J. Pan, B. Huang, C. Ren and D. Zeng, *J. Taiwan Inst. Chem. Eng.* 45 (2014) 1918
4. K. R. Ansari, M. A. Quraishi, A. Singh, S. Ramkumar and I. B. Obote, *RSC Adv.* 6 (2016) 24130
5. S. Shahabi and M. Reza, *RSC Adv.* 5 (2015) 20838
6. A. A. Farag, A. S. Ismail and M. A. Migahed, *J. Mol. Liq.* 211 (2015) 915
7. J. Kim, K. Tak and I. Moon, *Ind. Eng. Chem. Res.* 51 (2012) 10191
8. M. Yadav, D. Behera, S. Kumar, R.R. Sinha, *Ind. Eng. Chem. Res.* 52 (2013) 6318
9. M. Yadav, D. Behera, U. Sharma, *Corros. Eng. Sci. Technol.* 48 (2013) 19
10. M. Yadav, D. Behera, U. Sharma, *Arab. J. Chem.* (2012)<http://dx.doi.org/10.1016/j.arabjc>
11. M. Yadav, U. Sharma, *J. Mater. Environ. Sci.* 2 (2011) 407
12. K.D. Neemla, A. Jayaraman, R.C. Saxena, A.K. Agrawal, R. Krishna, *Bull. Electrochem.* 5 (1989) 250
13. M.A. Quraishi, N. Sardar, H. Ali, *Corrosion* 58 (2002) 317
14. S. Vishwanatham, P.K. Sinha, *Anti-Corros. Methods Mater.* 56 (2009) 139
15. H.A. Sorkhabi, B. Shaabani, D. Seifzadeh, *Electrochim. Acta* 50 (2005) 3446

16. M.M. Singh, S. Banerjee, V. Srivastava, *Corros. Sci.* 59 (2012) 35
17. H.L. Wang, H.B. Fan, J.S. Zheng, *Mater. Chem. Phys.* 77 (2002) 655
18. S. Tamilselvi, V. Raman, N. Rajendran, *J. Appl. Electrochem.* 33 (2003) 1175
19. Q.B. Zhang, Y.X. Hua, *Electrochim. Acta* 54 (2009) 1881
20. F. Bentiss, M. Lebrini, H. Vezin, M. Lagrenee, *Mater. Chem. Phys.* 87 (2004) 18
21. R. Solmaz, G. Kardaş, M. Çulha, B. Yazici, M. Erbil, *Electrochim. Acta* 53 (2008)
22. A.S. Yaro, A.A. Khadom, H.F. Ibraheem, *Anti-Corros. Methods Mater.* 5 (2011) 116
23. A.S. Yaro, A.A. Khadom, R.K. Wael, *Alexandria Eng. J.* 52 (2013) 129
24. M. Hazwan, M. Hussin, M. Jain, Kassim, *Mater. Chem. Phys.* 125 (2011) 461
25. K.H. Hassan, A.A. Khadom, N.H. Kurshed, *South Afr. J. Chem. Eng.* 22 (2016) 1
26. R.S. Nathiya, R. Vairamuthu, *Egypt. J. Petroleum* 26 (2017) 313
27. K. Krishnaveni, J. Ravichandran, A. Selvaraj, *Acta Metall. Sin.* 6 (2003) 321
28. B.S. Audu, P.C. Ofojekwu, A. Ujah, M.N.O. Ajima, *J. Phytol.* 3(2014) 35
29. N. Chaubey, D. K. Yadav, V. K. Singh, M.A. Quraishi, *Ain Shams Eng. J.* 8 (2017) 673
30. A.C.G.-o.C.o. Metals, Standard practice for preparing, cleaning, and evaluating corrosion test specimens, ASTM international 2017.
31. M. Frisch, G. Trucks, H. Schlegel, G. Scuseria, M. Robb, J. Cheeseman, G. Petersson. (2009). Gaussian 09 Revision D. 01, Gaussian Inc. Wallingford CT.
32. Materials Studio 6.1 Manual, Accelrys Inc., San Diego, CA, 2007
33. M. Yadav, Debasis Behera, Usha Sharma, *Arab. J. Chem.*, 9 (2016) S1487.
34. Akhil Saxena, Dwarika Prasad, Rajesh Haldhar, Gurmeet Singh, Akshay Kumar, *J. Mol. Liq.*, 258 (2018) 89.
35. Liu Li Liao, Shi Mo, Hong Qun Luo, Nian Bing Li, *J. Colloid Int. Sci.*, 520 (2018) 41.
36. A. Singh, K. Ansari, Y. Lin, M. Quraishi, H. Lgaz, I.-M. Chung, *J. Taiwan Inst. Chem. E.* 95 (2019) 341
37. A. Singh, K. Ansari, M. Quraishi, H. Lgaz, *Materials*, 12 (2019) 17.
38. S. Manimegalai, P. Manjula, *J. Mater. Environ. Sci.* 6 (2015) 1629
39. A. Singh, K.R. Ansari, M.A. Quraishi, S. Kaya, P. Banerjee, *New J. Chem.* (2019) DOI: 10.1039/c9nj00356h
40. N. Yilmaz, A. Fitoz, K.C. Emregül, *Corros. Sci.* 111 (2016) 110
41. M. ElBelghiti, Y. Karzazi, A. Dafali, B. Hammouti, F. Bentiss, I. Obot, I. Bahadur, E. Ebenso, *J. Mol. Liq.* 218 (2016) 281
42. M. Tourabi, K. Nohair, M. Traisnel, C. Jama, F. Bentiss, *Corros. Sci.* 75 (2013) 123
43. S.S. Abdel-Rehim, K.F. Khaled, N.A. Al-Mobarak, *Arabian J. Chem.* 4 (2011) 333
44. A. Singh, K.R. Ansari, A. Kumar, W. Liu, C. Songsong, Y. Lin, *J. Alloys Compd.* 712 (2017) 121
45. A. Singh, K. R. Ansari, M. A. Quraishi, H. Lgaz, *Materials* 2019, 12, 17; doi:10.3390/ma12010017
46. M. Salman, K.R. Ansari, V. Srivastava, D. S. Chauhan, J. Haque, M.A. Quraishi, *J. Mol. Liq.* 322 (2021) 114825